



PERGAMON

International Journal of Impact Engineering 24 (2000) 809–820

INTERNATIONAL
JOURNAL OF
IMPACT
ENGINEERING

www.elsevier.com/locate/ijimpeng

Chain composites under ballistic impact conditions

B.N. Cox^{a,*}, N. Sridhar^a, J.B. Davis^a, A. Mayer^b, T.J. McGregor^b, A.G. Kurtz^b

^aRockwell Science Center, 1049 Camino Dos Rios, Thousand Oaks, CA 91360, USA

^bWright-Patterson Air Force Base, Dayton, OH 45433, USA

Received 16 October 1999; received in revised form 13 December 1999

Abstract

An existing family of composites of steel chains in resin matrices that exhibit delocalized failure and high levels of energy absorption under static tensile loading has been tested under high-velocity impact conditions. Panels of chain composites were shot with anti-personnel rounds in an instrumented test range. The tests demonstrate that the lockup mechanism operates at strain rates approaching 10^4 s^{-1} , with delocalized damage extending in several cases from the impact site to the edge of the test panel. Estimates of the energy absorbed per unit volume under impact conditions range from 30 to 75 MJ/m², approximately 50–60% higher than values measured in static tension for the same composites. The enhancement of energy absorption is tentatively attributed to strengthening of the resin at high strain rates. Implications of the tests for designing ballistic protection are discussed. © 2000 Elsevier Science Ltd. All rights reserved.

1. Introduction

Many energy absorption problems involve loads that are tensile, for example casings designed to contain bursting rotors, turbines, or flywheels; backing plates in armour systems; and containers subject to internal explosions. Here some results of ballistic tests are shown for a new class of chain composites with unusually high energy absorption capacity under tensile loading.

The chain composites incorporate mechanisms for ensuring that damage is broadly distributed throughout the body of a specimen or structure before the instability associated with ultimate failure sets in [1]. Damage delocalization is promoted by the presence of a so-called lock-up mechanism, in which chain links are arrested by physical contact with one another after displacing through the matrix. The extent of the displacement allowed before the lock-up of two links determines the global engineering strain up to which damage will remain delocalized, which is

* Corresponding author.

E-mail address: bncox@rsc.rockwell.com (B.N. Cox).

denoted ε_c . The total energy absorbed per unit volume is bounded from below by the product of ε_c and the magnitude of the global composite engineering stress required for reinforcement displacement, σ_d . Measured levels of total energy absorbed per unit volume by chain composites in static tests range up to 60 MJ/m^3 . The potential for levels up to 180 MJ/m^3 in optimized chain composites has been demonstrated by modeling the micromechanics of link displacement [2,3].

Here static tests are extended to the dynamic regime (local strain rates $\sim 10^4 \text{ s}^{-1}$) by a series of ballistic tests on flat panels of chain composite. The essential questions addressed in the tests are whether lockup and the delocalization mechanism will be activated at high strain rates and what levels of energy absorption per unit volume can be achieved under dynamic conditions.

2. Composites of chains under static loading

Composites of chains in epoxy matrices in which the links are initially in a contracted configuration (Fig. 1) fail under static loading with damage spread over the whole stressed volume. The underlying phenomena were first discussed in [1] and have now been analyzed quantitatively by analytical and computational methods [2,3]. Damage begins with extensive matrix cracking. Successive chain links slide towards contact with one another, crushing resin trapped between them in a state of near hydrostatic compression. The displacement of links through the resin absorbs most of the energy expended en route to ultimate failure. When two links come into direct contact, they are said to lock up: the material hardens locally, resisting further local displacement

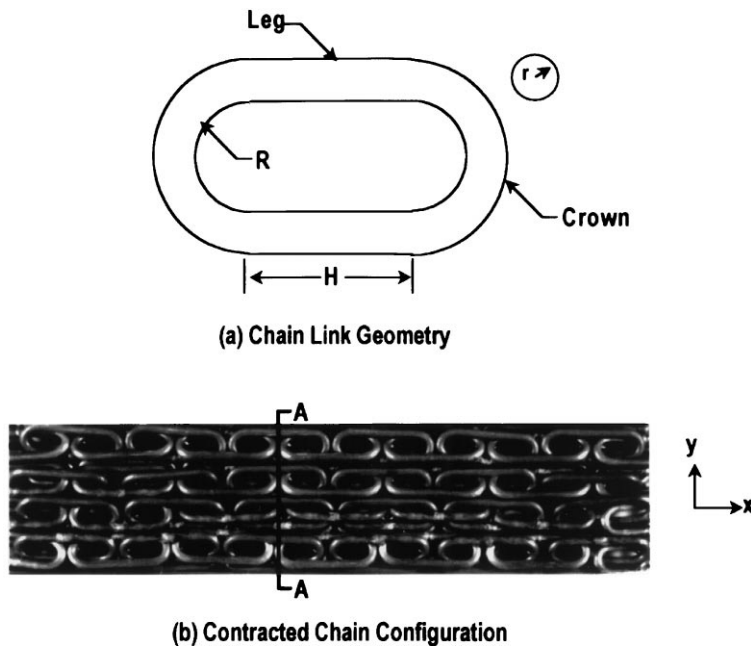


Fig. 1. (a) Notation for the geometry of a common racetrack-shaped link. (b) Links laid up in a chain composite in the contracted configuration, viewed through a transparent epoxy matrix.

and triggering the displacement of links elsewhere in the same chain. Only when all links in a chain are in direct contact with their neighbors does the chain begin to fail by plastic deformation of the links followed by rupture of the weakest among them.

A typical stress–strain curve from a static test is shown in Fig. 2. During link displacement, the applied engineering stress is approximately constant in most chain/polymer composites (strain less than 0.5 in Fig. 2). Its magnitude can be estimated by modeling the matrix as a rigid/perfectly plastic medium through which the links must move. Stress transfer into the links from the matrix during the displacement can be partitioned conveniently into several contributions. (1) Hydrostatic compression in the resin trapped between two links as they approach one another exerts pressure over the inner surface of the crown of each link (the curved end). (2) Shear tractions develop over the crown of a link as it slides through the matrix. (3) Tensile tractions act on the outer surface of the crown where the matrix is being pulled apart between the crowns of abutting links, at least until the matrix fails (e.g., along line A–A in Fig. 1). (4) Shear stresses act over the legs (the straight portions) as the links slide through the matrix. The sum of the four contributions, when resolved in the direction of the motion of the links, must be balanced by tension in the legs, which takes its maximum value, $\sigma_{\max}^{(\text{leg})}$ at the center of the legs; and all four are proportional to the matrix shear flow stress, σ_{my} , the constants of proportionality depending on the link geometry. Summarizing the results of finite element calculations [2]

$$\sigma_{\max}^{(\text{leg})} = \beta \sigma_{my},$$

$$\beta \equiv \frac{2}{\pi} (C_1 + C_2 + 3.664C_3) \left(1 + \frac{R}{r}\right) - \left(\frac{C_1 - C_2}{2}\right) + C_4 \frac{H}{r}, \tag{1}$$

where r is the radius of the wire in the link, R is the inner radius of the crown segment, H is the length of the leg segment (Fig. 1a), and C_1 , C_2 , C_3 , and C_4 are dimensionless constants of proportionality corresponding in order to the four contributions listed above. Eq. (1) is restricted to

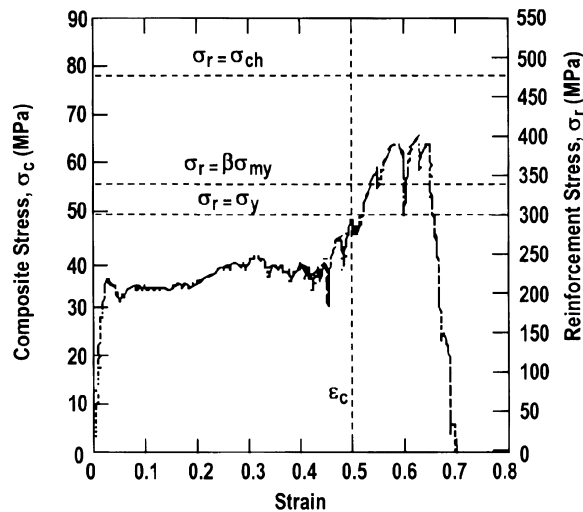


Fig. 2. Stress–strain record from a static test of a composite of carbon steel chains in an epoxy matrix (small links; data from [3]).

links consisting of semi-toroidal crowns connected by cylindrical legs, which is the standard geometry of commercially available chains. Analytical estimates for this geometry yield $C_1 \approx 1 + \pi/2$; while $C_2 \approx 1$ and $C_3 = C_4 \approx 1/2$ for perfectly bonded link/matrix interfaces; and $C_2 = C_3 = C_4 = 0$ for debonded, frictionless interfaces [2]. Finite element calculations of the interaction of a link and a perfectly plastic matrix yield for perfectly bonded interfaces the more accurate but still simple result [2]

$$\beta = 2.37 + 3.32 \frac{R}{r} + 0.5 \frac{H}{r} \quad (2)$$

and for unbonded, frictionless interfaces

$$\beta = 0.36 + 1.69 \frac{R}{r}. \quad (3)$$

Eq. (3) represents the case that the dominant resistance to link displacement arises from the matrix trapped under hydrostatic compression acting on the crown of the link. This is the situation in the epoxy/steel chain composites fabricated to date [3].

If the matrix is relatively compliant, then Eq. (1) multiplied by the area fraction occupied by the legs of the links on a plane through their centers (e.g., the plane A–A in Fig. 1) should be approximately equal to the composite stress during link displacement, σ_d . This is shown in Fig. 2 by the line marked “ $\sigma_r = \beta\sigma_{my}$ ”. It is a little above the measured plateau stress. The discrepancy is attributed to loss of matrix from the composite, which reduces the resistance to link displacement and was not included in the model. In static tests, the matrix fractures into fairly small pieces, which are ejected from the specimen at intermediate strains.

A transition from delocalized to localized failure should occur if $\sigma_{max}^{(leg)}$ exceeds the strength of the chain material, σ_{ch} , during link displacement. This was not the case in the test of Fig. 2. However, when the composite stress divided by the area fraction of the links, which is denoted σ_r , exceeds σ_{ch} following link lockup, the chains must fail. This condition is indicated by the line marked “ $\sigma_r = \sigma_{ch}$ ” in Fig. 2. The line lies somewhat above the measured peak stress, a discrepancy attributed to slightly unequal loading among the chains.

3. Ballistic impact tests of chain composite panels

3.1. Test panels

Specimens were made with carbon steel chains of two sizes, whose specifications are listed in Table 1. The listed static ultimate strengths of the chains were measured as the load to failure divided by the cross-sectional area of the two legs of a link. Square panels were fabricated with lateral dimensions approximately 127×127 mm. The chains were laid up in two layers in the contracted configuration illustrated by Fig. 1b, with the chain orientation alternating between 0 and 90° from layer to layer. Four panels, whose specifications are listed in Table 2, were tested. The chains were set in Epofix epoxy resin. The listed volume fraction of the chains was deduced from the measured total panel mass and the known densities of carbon steel and epoxy resin. They

Table 1
Chain and resin specifications

	H (mm)	R (mm)	r (mm)	Static ultimate strength σ_{ch} (MPa)	Static yield strength σ_y (MPa)	Density ρ (mg/m ³)
Small link	8.67	1.79	0.955	480	300	7.9
Large link	21.75	3.00	1.5	460	300	7.9
Epoxy resin					100 ^a	1.60

^aUltimate compressive strength at room temperature — *Engineered Materials Handbook, Vol. 1., Composites.*

Table 2
Data from ballistic tests

Specimen label	Chain link size	Panel thickness t (mm)	Volume fraction of chains	Impactor mass m (gm)	Incident velocity v_{in} (m/s)	Exit velocity v_{out} (m/s)	Energy loss ΔK (J)	Fractional energy loss
CA #1	Small	9.4	0.30	10.5	344	15	620	0.998
CA #2	Small	9.4	0.30	10.5	332	102	523	0.91
CA #3	Large	16.3	0.20	44.9	337	152	2033	0.80
CA #4	Large	16.0	0.22	45.2	236	52	1197	0.95

are higher for the panels made with small links because the links were packed more skillfully in these panels. The areal densities of the chain composites were approximately 0.032 g/mm² for the small link panels and 0.047 g/mm² for the large link panels. Plates of monolithic steel of the same areal density as the small and large link panels would be 4 and 6 mm thick, respectively.

3.2. Ballistic test procedure and observations

The panel specimens were tested under impact by 0.30 and 0.50 calibre armour piercing (AP) rounds fired from a gun. The rounds are made of lead with a copper jacket and are pointed. Each specimen was clamped around its periphery in a square gripping arrangement. The panels were milled in the gripped region to expose chain links for better load transfer.

The incident velocity for which the probability of penetration for the chain composites would be expected to be 0.5 was estimated by testing mild steel plates of similar areal density. Tests of the chain composites were then conducted at around this incident velocity.

The round achieved penetration in every test, with incident and exit velocities, v_{in} and v_{out} , and kinetic energy lost from the round, ΔK , as listed in Table 2. The fractional energy loss shown in Table 1 is defined as the ratio of the listed energy loss to the incident kinetic energy of the round. The rounds were not severely damaged by the tests, implying that most of the lost kinetic energy went into deformation of the chain composite rather than of the round itself.

Representative states of damage of a chain composite panel following a test are shown in Fig. 3. On both faces, chains have failed. The failed links and a number of links on either side in the same chains have been displaced to the point of lockup. This process is generally much more widespread

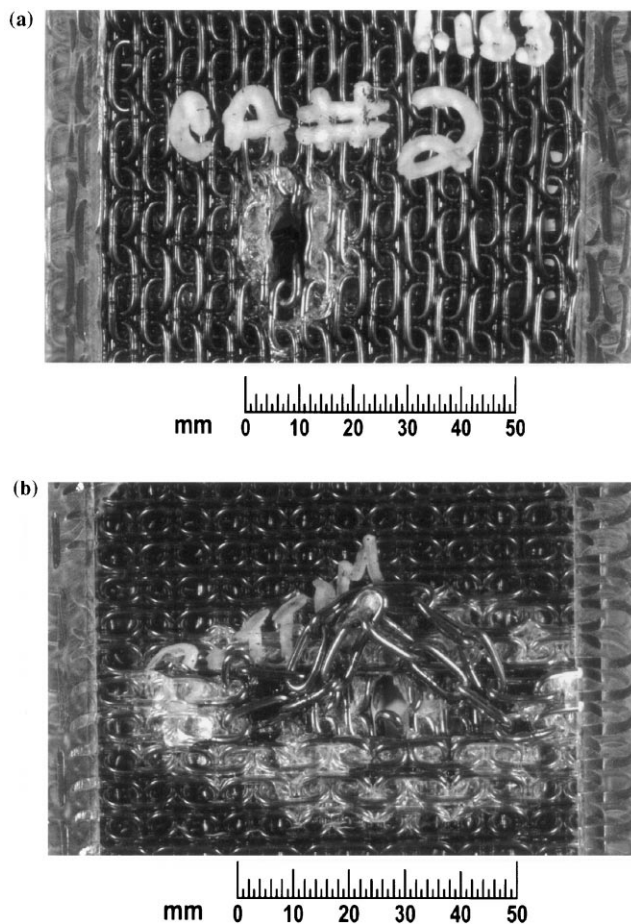


Fig. 3. Chain panel made from small link chains after passage of a round. (a) Incident face. (b) Exit face.

on the exit face, being confined to the environs of the impact site on the incident face. In the specimen shown, more distant damage on the front face consists solely of distributed matrix cracks and accounts for a minor contribution to energy absorption. On the rear (exit) face, links are significantly displaced all the way to the edge of the plate. In one case, specimen CA #4, two chains were pulled completely out of the gripping area at the specimen's edge.

High-speed photography showed resin ejected from both the incident and exit faces. Links were seen flopping quite freely against the exit face once they had been freed from the resin.

4. Deformation of the chain composite during impact

Energy absorption in the chain composites is associated primarily with the very high levels of damage to resin that occurs when links displace through it all the way to lockup. This is evidenced by the stress-strain record under static loading. Distributed matrix cracking similar to that in Fig. 3

(white zone below impact site in Fig. 3b and minor cracking more remote from the impact site, which is difficult to see in the photographs) occurs in static tests at quite low strains (~ 0.01 – 0.05), yet the global stress during this phase is no higher than during the subsequent displacement of links to lockup (Fig. 2). Therefore, the energy dissipated in this cracking (area under the stress–strain curve) is relatively small. In contrast, the displacement phase of damage lasts from strains of near zero to strains of approximately 0.5 and occurs at much the same stress levels. Thus, the plastic work done against the matrix during link displacement is much larger than the energy associated with distributed matrix cracking; and it will also be much larger than the energy dissipated in elastic wave propagation. The most important issue is therefore to quantify the process of link displacement. Links that have been displaced significantly towards lockup will be said to have been activated. In the following, some estimates of the energy absorption in the activated chains are made, based on the assumption that all of the kinetic energy lost from the round has gone into displacing activated links.

To characterize the energy-absorbing damage in a panel, the distribution of displacements of individual links was tabulated by inspection of the panels after ballistic testing. The displacement of any link was recorded as a fraction, ϕ_d , of the displacement required for its lockup against the next link in the chain. If all resin was missing between the two links, ϕ_d was recorded as unity: lockup was assumed to have been achieved. If two links had displaced significantly but not to lockup, they were assigned a fractional displacement $\phi_d = 0.5$. This two-valued approximation for ϕ_d is adequate for estimating the total energy absorbed, which is the sum over all links — errors in characterizing individual link displacements tend to cancel. The recorded numbers of links $n_{0.5}$ or n_1 with $\phi_d = 0.5$ or 1 are shown for each specimen in Table 3. Two-thirds to three-quarters of the activated links lay in the rear layer of chains.

The round will be assumed to have dragged the chains it contacted during impact out away from the panel (Fig. 4). To accommodate this chain displacement, the links within the chains must have displaced towards lockup. Since activation sometimes extends only part of the way to the specimen boundaries in some specimens, activation is inferred to have begun at the site of impact and propagated away from it, with successive links locking up fully before the next link began to be

Table 3
Estimates of kinematic characteristics of impact

Specimen label	CA # 1	CA # 2	CA # 3	CA # 4
Number of links with $\phi_d = 1$	12	13	13	15
n_1				
Number of links with $\phi_d = 0.5$	0	12	2	3
$n_{0.5}$				
Maximum number of locked up links in one chain	3	3	2	2
n				
Interval of contact d (mm)	28	28	44	44
Angle θ (deg)	49	49	53	53
Energy partition $\Delta K_{\text{rear}}/\Delta K$	0.74	0.74	0.71	0.64
Time of contact t_0 (ms)	0.18	0.14	0.20	0.36
Lockup strain ϵ_c	0.52	0.52	0.64	0.64
Max. velocity of front v_f (m/s)	257	252	227	146
Max. strain rate $\dot{\epsilon}$ (s^{-1})	8380	8220	4330	2790

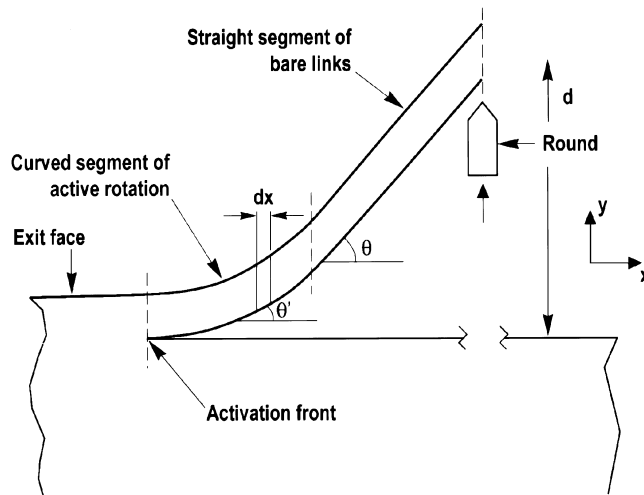


Fig. 4. Schematic of the drawing of activated chains from the panel by a passing round.

displaced. Because the chains are held into the composite by resin only, which is brittle and weak in tension, the activated links can rotate relatively easily between the activation front and the impactor, as shown in Fig. 4. The rotation will be assumed to have occurred within a relatively small interval. (Links and resin in this curved section could be represented as a beam, in which large membrane tension exists, along with such bending moments and shear as are required to support the curvature.) When the links have displaced fully to lockup, the resin will have been ejected from their vicinity, leaving bare links in contact to sustain load. These bare links must lie on a straight line, as indicated in Fig. 4. The angle of the straight line to the back face of the plate, θ , is related to the strain to lockup, ε_c . It is constant during propagation of the activation zone if the curved segment is small.

4.1. Kinematics

Here a simple geometric analysis based on the depiction of events just described is used to estimate key velocities and the strain rate. The kinematic analysis will address the interaction of the round with the rear layer of chains, which are free to deform in the assumed manner. The kinetic energy lost by the round (Table 2) can be partitioned into energy absorbed by the front and rear layers of chains in proportion to the number of activated links in the layers. The ratio of the energy absorbed in the rear layer to the total energy absorbed, $\Delta K_{\text{rear}}/\Delta K$, is listed in Table 3. It lies between $\frac{2}{3}$ and $\frac{3}{4}$. From this energy partition, the incident velocity for the round upon the rear layer of chains, v_2 , can be estimated as

$$\frac{v_2^2 - v_{\text{out}}^2}{v_{\text{in}}^2 - v_{\text{out}}^2} = \frac{\Delta K_{\text{rear}}}{\Delta K}. \quad (4)$$

Let t_0 denote the time of contact between the round and the activated chains in the rear layer, d the interval of the round's flight through which contact exists, m the mass of the round, and F the force

acting on the round. If the loads in the locked-up chains and the angle θ are constant during propagation of the activation zone, then F and the rate of deceleration of the round must also be constant. Then

$$t_0 = \frac{2d}{v_2 + v_{\text{out}}}. \quad (5)$$

Denote by n the greatest number of links in any chain that are activated and attain lockup, counting from the impact site in one direction only. The initial length of the n links in the pristine composite is

$$s_1 = \frac{n}{2}[H + 2(2r + R)] \quad (6a)$$

and the final length (after displacement to lockup) is

$$s_2 = n[H + 2R], \quad (6b)$$

where H , R , and r are defined in Fig. 1. Thus, the engineering strain to lock-up is

$$\varepsilon_c = \frac{s_2 - s_1}{s_1} = \frac{H/r + 2R/r - 4}{H/r + 2R/r + 4}. \quad (7)$$

The interval of contact is

$$d = n[s_2^2 - s_1^2]^{1/2}, \quad (8)$$

while the angle of deflection of the activated chains is

$$\theta = \cos^{-1} \left[\frac{s_1}{s_2} \right]. \quad (9)$$

The activation front advances with a velocity, v_f , that is in direct proportion to the velocity of the round, v_r , during contact

$$v_f = \frac{v_r}{\sqrt{(1 + \varepsilon_c)^2 - 1}}. \quad (10)$$

Thus, v_f has its maximum value, v_0 , at the initiation of contact and decreases linearly thereafter.

Inspection of impacted specimens shows that where the activation front has not reached the specimen boundary, links on the impact side of the front are fully displaced to lockup, while links to the other side are barely displaced at all. Therefore, the progression of a link from first entering the activation zone to being free of resin and fully locked up occurs when the activation front moves over a distance comparable to the length of one link. The average strain rate during this process must be

$$\dot{\varepsilon} = \frac{\varepsilon_c v_f}{[H + 2(R + 2r)]}, \quad (11)$$

which again has its maximum value at the initiation of contact. Peak values of $\dot{\varepsilon}$ approach 10^4 s^{-1} .

The maximum number of locked up links, n , observed in any chain on the exit side of the panel (where most locked up links are found) is listed in Table 3 along with ensuing estimates of various kinematic parameters. The interval of contact and the contact time are inferred directly from n . The maximum (initial) velocity of the activation front and the maximum strain rates depend mainly on the velocity data of Table 2 and only weakly on the count of activated links, which enters through the energy partitioning step.

4.2. Energy absorption

If all the kinetic energy lost by the round, ΔK , is assumed to be taken up by work done in displacing all activated links (front and rear layers), then the energy absorbed per unit volume by the chain composite in the activated zone, W , is just the ratio of ΔK to the initial volume of the activated zone, V_a . In a tightly packed array of chains, each chain occupies an area perpendicular to its axis given by [3]

$$A = \left[2r + 2(r + R) \cos \frac{\alpha}{2} \right] \left[2r + 2(r + R) \sin \frac{\alpha}{2} \right], \quad (12a)$$

where

$$\alpha = \sin^{-1} \left[\frac{2r}{r + R} \right] \quad (12b)$$

and, in the initial contracted chain configuration, each link accounts for a length

$$l_1 = \frac{1}{2} [H + 2(2r + R)]. \quad (12c)$$

Thus,

$$W = \frac{\Delta K}{V_a} = \frac{(m/2)(v_{in}^2 - v_{out}^2)}{NA[H + 2(2r + R)]} \quad (13a)$$

with the assignment

$$N = n_1 + n_{0.5}/2 \quad (13b)$$

which gives a fair representation of the apportioning of energy absorption to fully and partially activated volumes. Values of W estimated for the four tests are listed in Table 4, along with the equivalent quantity, $W^{(st)}$, from static tests [3]. The energy absorbed per unit volume is approximately 50–60% higher in dynamic tests than in static tests for all but specimen CA #4, where the static value is slightly higher. In this test, activated chains pulled free from the grip region of the specimen, so that energy absorption was interrupted.

4.3. Peculiarities of dynamic damage propagation

Possible reasons for the energy absorption levels inferred for dynamic loading being higher than for static loading include the following. (1) At high strain rates, the yield stress of the epoxy resin matrix under conditions of hydrostatic compression (resin trapped between links) rises. Data from

Table 4
Energy absorption and macroscopic stresses in activated chains

	Energy absorption in activated zone W (MJ/m ³)	Energy absorption in static loading $W^{(st)}$ (MJ/m ³)	Force on impactor F (kN)	Load in chains when $\theta' = \theta$ F_{ch} (kN)	Area of chain A (mm ²)	Composite stress in activated zone σ_c (MPa)	Plateau stress in static loading $\sigma_c^{(st)}$ (MPa)
CA #1	73	44	11.2	3.71	27.8	133	40
CA #2	62	44	14.2	4.70	27.8	169	40
CA #3	61	38	52.9	12.67	70.9	179	35
CA #4	30	38	31.2	7.47	70.9	105	35

[4] show that both the shear yield strength (corresponding to relatively small shear strains) and the shear strength of epoxy resins approximately double at strain rates of $\sim 10^4 \text{ s}^{-1}$ relative to static loading values. Simultaneously, the ultimate strength of the steel links will rise with strain rate [5,6], so that the links remain strong enough to be dragged through the increasingly resistant resin. (2) At high strain rates, the time required for resin fragments to be ejected from the region of entrapment between links may be comparable to the time of the link displacement ($< 10^{-4} \text{ s}$ for a single link to reach lockup). (3) In the static tests cited for comparison, the applied load was uniaxial. In the impact experiments, activated chains rotate as well as extending. Additional work might be expected to be absorbed during link rotation.

Thus, optimal design of chain composites for impact resistance must be based on material properties that may be significantly different from those found for static loading. Tests that are more amenable to analysis than the ballistic tests reported here, both in regard to mechanisms and stress distributions, need to be developed to acquire the necessary data.

5. Concluding remarks

Ballistic tests show that the mechanisms of link displacement, lockup, and damage delocalization persist in chain composites at strain rates approaching 10^4 s^{-1} . Activation zones of links that have displaced to lockup can extend to the edge of the tested plate. Energy absorption is thus spread over a much larger volume of material than in ballistic impact upon monolithic materials or conventional composites. Estimates of the energy absorbed per unit volume in the activated zones yield levels 50–60% higher than measured in static tension tests of similar chain composites. In static tests, the stress required to displace links through the resin and therefore the energy absorbed are proportional to the flow stress of the resin (Eq. (1)). Thus, the greater energy absorption under dynamic conditions may be due to a higher flow stress in the resin at high strain rates under conditions of nearly hydrostatic compression. It may also be attributed in part to reduction of resin ejection, which can lead to premature loss of resistance to link displacement, under dynamic conditions.

The tests reported here should be regarded as a demonstration of the lockup mechanism at high strain rate and not as a quantitative assessment of the performance of chain composites as ballistic protection. In their current configuration, the chain panels have several obvious limitations as ballistic protection. Contact between the round and the activated chains tends to be interrupted by

the round breaking the contacted links or slipping through or past them. This terminates propagation of the activated zone and the deceleration of the round. Activation is also restricted mainly to the rear layer of chains, which have the freedom to extend into the free space behind the plate, allowing an activated zone to develop. Chains in the front layers are constrained by the layers behind them and exhibit far smaller activation zones.

These problems can be remedied by simple redesign. For example, persistent contact between links and the round can be achieved by using smaller links, with smaller holes and a higher density of chains per unit width of the panel. To first order under static loading, the lockup strain and the stress required for link displacement are invariant under changes of scale that preserve similarity [2], since both depend only on ratios of dimensions (Eqs. (1) and (7)). Therefore, the energy absorption per unit volume or mass must be invariant too. Round penetration can also be combated by generalizing the shape of the links. Space filling links, topologically equivalent to racetrack links but presenting nearly gapless, prismatic outer surfaces, can be considered [7]. Alternatively, a hard plate or a set of hard tiles can be placed in front of the chains to flatten the projectile and spread loads over a larger area of the chain panel, ensuring greater activation of links.

Better use of multiple layers of chains will presumably be achieved if the layers are separated in space, so that each layer can be activated without constraint from succeeding layers. The spacing of layers should be enough to accommodate the chain deflection depicted in Fig. 4. Multiple layers separated by layers of light polymer foam would seem an attractive option. Matrix ejection can be reduced by using more ductile matrices, such as polycarbonate or elastomers.

The chain concept can clearly be generalized to arrays of links coupled in two dimensions, rather than as one-dimensional chains. The chain reinforcement would then bear superficial resemblance to chain mail. However, the ductility of chain mail arises primarily from plastic deformation of the links, together with some frictional resistance to limited link sliding. Here, in contrast, the major component of the work of deformation is expended in the matrix before the links come into contact and begin to change shape. The essence here is to match the strength of the links to the resistance of the matrix to link displacement.

Acknowledgement

Work supported by the US Army Research Office, Contract no. DAAH04-95-C-0050.

References

- [1] Cox BN. Lockup, chains and the delocalization of damage. *J Mater Sci* 1996;31:4871–81.
- [2] Gong X-Y, Zok F, Cox BN, Davis J. The mechanics of delocalization and energy absorption in chain composites. *Acta Mater*, in press.
- [3] Cox BN, Davis J, Sridhar S, Zok F, Gong X-Y. The energy absorption potential of chain composites. *Acta Mater*, in press.
- [4] Miwa M, Takeno A, Yamazaki H, Watanabe A. Strain rate and temperature dependence of shear properties of epoxy resin. *J Mater Sci* 1995;30:1760–5.
- [5] Campbell JD, Ferguson WG. *Philos Mag* 1970;21:63.
- [6] Meyers MA. *Dynamic behaviour of materials*. New York: Wiley, 1994.
- [7] Cox BN. Space-filling chain composites for energy absorption. Unpublished work.